Recurrent large-scale solar proton events before the onset of the Wolf grand solar minimum

Hiroko Miyahara[1], Fuyuki Tokanai[2], Toru Moriya[2], Mirei Takeyama[2], Hirohisa Sakurai[2], Motonari Ohyama[3], Kazuho Horiuchi[4], and Hideyuki Hotta[5]

[1]Humanities and Sciences/Museum Careers, Musashino Art University
[2]Yamagata University
[3]Tohoku University
[4]Hirosaki University
[5]Department of Physics, Graduate School of Science, Chiba University

November 23, 2022

Abstract

Carbon-14 in tree rings have suggested that there had been multiple extreme solar proton events (SPEs) in the past. While the largest events such as in 774–775 CE can be significantly detected by the typical precision of accelerator mass spectrometry, smaller but possibly more frequent events have been difficult to be detected. Thus, the frequency or any characteristics of such relatively smaller events are still largely unknown. In this paper, we report that multiple large SPEs had occurred before the onset of the Wolf grand solar minimum based on high-precision carbon-14 analyses. It is suggested that they had occurred at the maximum and the declining phase of solar cycles, and that they had occurred during the transition time of solar activity into a deep minimum. We propose that this episode may provide a unique opportunity to elucidate a potential interaction between the solar dynamo and extreme solar flares.

Recurrent large-scale solar proton events before the onset of the Wolf grand solar minimum

Hiroko Miyahara[1,2,*], Fuyuki Tokanai[3,4], Toru Moriya[4], Mirei Takeyama[4], Hirohisa Sakurai[3], Motonari Ohyama[5], Kazuho Horiuchi[6], and Hideyuki Hotta[7]

[1]Humanities and Sciences/Museum Careers, Musashino Art University, Tokyo 187-8505, Japan.

[2] Okinawa Institute of Science and Technology Graduate University, Okinawa 904-0495, Japan

[3]Faculty of Science, Yamagata University, Yamagata 990-8560, Japan.

[4]Center for Accelerator Mass Spectrometry, Yamagata University, Yamagata 999-3101, Japan.

[5]Botanical Gardens, Tohoku University, Miyagi 980-0862, Japan

[6]Graduate School of Science and Technology, Hirosaki University, Hirosaki, Aomori 036-8561, Japan.

[7]Department of Physics, Graduate School of Science, Chiba University, 1-33 Yayoi-cho, Inage-ku, Chiba 263-8522, Japan.

*Correspondence to miyahara@musabi.ac.jp

Key points:

・Multiple abrupt increases in carbon-14 content were found during the transition time of solar activity into the grand minimum state

・They occurred at solar activity maximum or at the declining phase of solar cycles, suggesting that they originate from solar proton events

・The Wolf minimum may provide a unique opportunity to potentially deepen the understanding of the solar dynamo

Abstract

Carbon-14 in tree rings have suggested that there had been multiple extreme solar proton events (SPEs) in the past. While the largest events such as in 774–775 CE can be significantly detected by the typical precision of accelerator mass spectrometry, smaller but possibly more frequent events have been difficult to be detected. Thus, the frequency or any characteristics of such relatively smaller events are still largely unknown. In this paper, we report that multiple large SPEs

had occurred before the onset of the Wolf grand solar minimum based on high-precision carbon-14 analyses. It is suggested that they had occurred at the maximum and the declining phase of solar cycles, and that they had occurred during the transition time of solar activity into a deep minimum. We propose that this episode may provide a unique opportunity to elucidate a potential interaction between the solar dynamo and extreme solar flares.

1. Introduction

The Sun occasionally produces intense solar flares that sometimes accompany the ejection of energetic protons, described as solar proton events (SPEs). SPEs can potentially cause catastrophic damage to modern society by increasing the radiation levels around the Earth. For example, previous events have caused damage to spacecrafts (Shea et al., 1992) and increased the radiation exposure of airline crews and passengers (Fujita et al., 2021). Therefore, it is crucial to further understand how frequently and at which phases of solar activity large-scale SPEs may occur.

SPEs can be studied either by direct observation of cosmic-ray radiation or by obtaining proxy-based data such as carbon-14 content in tree rings and/or beryllium-10 stored in ice cores obtained from polar regions. Both carbon-14 and beryllium-10 are radioactive isotopes produced by incident cosmic rays in the atmosphere; thus, their content in tree rings or ice cores provides information on past cosmic-ray events (Lal and Peters, 1967). While these isotopes are constantly produced by galactic cosmic rays, whose flux is gradually changing due to variations of the solar-wind magnetic field with timescales of decade or longer, less energetic but massive radiations from SPE cause a rapid increase in their production rate.

Based on carbon-14 records, Miyake et al. (2012; 2013) reported two extremely large SPEs that occurred in 774–775 CE and 993–994 CE; the enhancement of carbon-14 content was approximately 1%, and both were detected by the ordinary precision of accelerator mass spectrometry (AMS) (0.2%–0.3%). Later, the enhancement of carbon-14 on a similar scale was also reported for 660 BC (O'Hare et al., 2019; Sakurai et al., 2020). For this event, detailed analyses have suggested that this peak might have been produced by multiple, successive SPEs occurring within a few years (Sakurai et al., 2020).

The frequency and the intensity of solar flares exhibit a power-law relationship (e.g., Figure 4 of Maehara et al., 2015); thus, large-scale but comparably smaller SPEs than 774–775 CE or 993–994 CE should have occurred more frequently in the past. However, it is difficult to detect such smaller events with carbon-14 in tree rings, as a transient enhancement in carbon-14 in the atmosphere is strongly attenuated in the carbon cycle. A few possible candidates have been found but are limited to those around 1052 CE and 1279 CE (Brehm et al., 2021), or around 5410 BC (Miyake et al., 2021).

Generally, SPEs occur when the Sun is active, as have been suggested for the 774–775 CE and 993–994 CE events; however, Brehm et al. (2021) have suggested that SPEs could also occur during grand solar minima when solar activity was extremely low for more than a few decades. During the grand minima, the number of sunspots emerging on the solar surface becomes extremely small; thus, there would be less chance for solar flares. However, it is known that sunspots had caused solar flares even during the Maunder Minimum (1645–1715 CE), one of the periods of extremely low sunspot activity, and had brought some aurorae events, although the event rate was extremely suppressed during that time (Schlamminger, 1990).

However, it should be noted that galactic cosmic rays (GCRs) may also cause an annual-scale rapid increase in carbon-14 around the grand minima (Yamaguchi et al., 2010; Kataoka et al., 2012). Such an event may occur at the minima of solar cycles during the grand solar minimum in the case where the current sheet in the heliosphere, which plays an important role in the modulation of cosmic rays, is extremely flattened. Such a condition may occur when the solar surface is quiet—without any active region—and thus the tilt of the neutral line on solar surface is reduced to ~0 degrees. Note that this effect is only prominent when the polarity of the solar dipole magnetic field is negative, which is when GCRs tend to come to the Earth along with the heliospheric current sheet by the drift effect (Kota and Jokipii, 1983). Thus, such an event may occur only at every other minima of solar cycles. The variation of beryllium-10 content obtained from ice cores has suggested that the polarity reversal of the solar magnetic field had been maintained even during the Maunder Minimum, with a slightly lengthened cycle, and that the GCR flux had been increased by 30%–40% at every other solar cycle minima (Yamaguchi et al., 2010; Kataoka et al., 2012).

Therefore, it is important to reconstruct the profile of solar cycles together with the cosmic-ray events so that their origin can be identified. The reconstruction of solar cycles also enables identifying the solar cycle dependence of large SPEs.

In order to determine the phases solar cycles at the times of cosmic-ray events, it is helpful to obtain high-precision carbon-14 data—better than 0.1% (Miyahara et al., 2021). Improving the measurement precision is also indispensable for detecting relatively small SPEs, as well as precisely determining their intensity to reveal their characteristics. In this paper, based on high-precision carbon-14 analyses, we report that multiple SPEs had occurred before the onset of the Wolf grand minimum that occurred in the late 13th to the early 14th century (Figure 1a). The solar cycle dependence of the events, as well as a possible relation to the grand minimum, are presented.

2. Materials and Methods

2.1. Measurement of carbon-14 content in annual tree rings

In this study, we used tree-ring samples of asunaro (*Thujopsis dolabrata*) excavated from the Shimokita Peninsula, Aomori Prefecture. Each of the annual tree rings were cross-dated by dendrochronology (Hakozaki, 2012) and absolutely dated by δ18O dendrochronology and carbon-14 spike-matching (Hakozaki et al., 2016). The tree rings formed in 1250–1295 CE were then separated and chemically treated to extract cellulose. We then produced graphite as a target material and measured the carbon-14 content using the AMS at Yamagata University in Japan (Tokanai et al., 2013; Moriya et al., 2019). In order to achieve high-precision, we prepared four cathodes from each of the cellulose samples, randomly loaded them onto the target wheel of the AMS, and repeated measurements of 300 s for 14–24 cycles. We duplicated such measurements two to three times to achieve a precision better than 0.08% in this study. We then calculated the Δ14C values following the methodology described in a previous study (Miyahara et al., 2021).

2.2. Estimation of carbon-14 production rate

For the determination of carbon-14 production rate, we used the 11-box carbon cycle model introduced by Güttler et al. (2015). We first calculated the steady state of the carbon cycle with the production rate of carbon-14 as 7.0 kg (total amount for the stratosphere and the troposphere) for 200 kyrs, and then continued the calculation for approximately 2000 years by adding a sinusoidal curve with a period of 4400 years to reproduce the variation in carbon-14 content (Reimer et al., 2020) caused by the long-term trend in geomagnetic field intensity.

The amplitude of the 4400-year cycle was adjusted so that the modeled $\Delta 14C$ value matched that of the measured value for the previous year of the cosmic-ray candidate event. We then estimated the production rate of carbon-14 that can reproduce the jump by injecting it into the model and by comparing the obtained carbon-14 content in the troposphere with the high-precision data. Note that the uncertainty of the carbon-14 data in the year before the event was propagated to that of the event year to estimate the production anomaly within a range of 1 σ. As any variations after the events may reflect decadal-scale solar activity variations, they were not considered for the estimation of the intensities of the events.

2.3. Reconstruction of solar cycles

In order to determine the profile of the solar cycles, we used a similar approach as described in Miyahara et al. (2021). We constructed possible synthetic curves of carbon-14 production rate caused by the decadal-scale variation of GCRs associated with solar cycles, inputted them into the 11-box carbon cycle model, and compared the modeled tropospheric carbon-14 content with the high-precision carbon-14 data obtained in this study. For this calculation, we slightly modified the initial setting mentioned in 2.2: the amplitude of 4400-year cycle was adjusted so that the modeled $\Delta^{14}C$ matched the measured value in 1250 CE.

For the construction of the synthetic curves, we first synthesized possible sunspot cycles and then obtained the corresponding cosmic-ray variations. For synthesizing the sunspot curves, we assumed that the length of the ascending phase did not exceed the length of the declining phase, following the characteristics of sunspot cycles during the past 300 years. We set the resolution of sunspot activity level as 20. For translating the sunspot cycles into cosmic-ray cycles, we utilized a simple model estimated based on the relationship between sunspot number and GCRs since 1953 CE as monitored by neutron monitors (Supplementary Figure S1). We normalized and combined the Climax neutron monitor data (http://cr0.izmir an.ru/clmx/main.htm) and the Oulu neutron monitor data (http://cosmi crays.oulu.fi/) and compared them with sunspot numbers for the two phases; the polarity of the solar dipole magnetic field was positive and negative, respectively (Supplementary Figure S1c). We obtained approximate equations and extrapolated the curves so that the calculation can be conducted for a wide range of solar activity levels. Note that the Sun sometimes indicates long-term variation in its magnetic activity not reflected in sunspot number, as was the case for the deep activity minimum in 2008–2009. We therefore extrapolated the curves down to a sunspot number of −150. As the decadal-scale variation in carbon-14 content around 1265–1277 CE was significantly suppressed compared to the previous/following cycle, we assumed that this cycle corresponded to a period when the solar dipole magnetic field was positive. Based on this assumption, we converted the sunspot curves into cosmic-ray variations.

We input the synthetic curves into the carbon cycle model cycle by cycle. At each cycle, $X^2 = \Sigma (\Delta^{14}C_{modeled} - \Delta^{14}C_{measured})^2/\sigma^2$ were calculated, and all the synthetic curves that resulted in an X^2 below 1.69 (σ = 1.3) were adopted to calculate the following cycle. As the obtained data do not fully cover the cycle ending around 1259 CE, and the profile of the solar maximum in the reconstruction may have a large ambiguity for this cycle, reconstructed curves are shown only from around 1255 CE. Note that the reconstructed sunspot activity level is dependent on the model of the GCR-sunspot relationship, especially above 270 and below 0; therefore, the levels of sunspot maxima and minima are reliable only in terms of relative magnitude.

3. Results and Discussion

Our newly obtained high-precision carbon-14 data, with a precision of 0.04%–0.08%, substantially improved the understanding of solar activity around the onset of the Wolf grand solar minimum in the 13th century. The data indicated that there were three abrupt cosmic-ray events in a relatively short period of time just before the onset of the Wolf minimum (Figure 1b). One of the events occurred in 1279–1280 CE, confirming one of the previously suggested SPE candidates by Brehm et al. (2021) (Figure 2a), although the high-precision data revealed that the increase in Δ14C was only approximately 0.3%, smaller than the 0.5% increase suggested by Brehm et al. (2021). Another event was found to have occurred in 1268–1269 CE (Figure 2b), 11 years before the above event. This event was larger than the 1279–1280 CE event, and the offset of Δ14C was approximately 0.45%. There was no increase from 1279 to 1280 CE in the Brehm's record; instead, a jump of similar scale is seen—although statistically insignificant—in the subsequent year. The discrepancy between the two records may be explained either by (1) the relatively large uncertainty of the record by Brehm et al. (2021) compared to the small signal or by (2) the tree species used to obtain the data. The asunao tree used in this study is a conifer that is known to start photosynthesis in early spring, and the majority of the produced photosynthate is used for growth during the same year. On the contrary, the oak used in the study of Brehms et al. (2021) is a deciduous tree that begins to sprout in May and defoliate in late October, in which case the photosynthate of the previous year is used for the growth of earlywood. It is therefore possible that the carbon-14 signal is delayed by one year in the case of the deciduous tree. A relatively small but possible SPE candidate was also found in the data in 1261–1262 CE. An increase of 0.24% (~3 σ) was found in the carbon-14 content together with a substantial decrease in 1263–1264 CE (Figure 2c), exceeding the level that can be explained by solar cycles.

It is suggested by the carbon cycle modeling that the production rate of carbon-14 caused by these three events was 5.6 ± 0.8 kg, 7.8 ± 1.2 kg, and 4.2 ± 1.4 kg, respectively (see Supplementary Figure S2), corresponding to ~19%, ~27%, and ~14% of the largest known SPE occurring in 774–775 CE (see Brehm et al., under review, for the production rate of the 774–775 event). The event in 1268–1269 CE had been suggested to have caused a 9.2 ± 2.4 kg increase in carbon-14 production rate (Brehm et al., 2021), but the high-precision data allowed for narrowing this uncertainty. The third event was the smallest extreme SPE candidate detected by carbon-14 so far with sufficient statistical significance, although further improvement in the measurement precision is desired for a better estimation of the intensity.

Figure 3 shows the evolution of solar cycles around the events calculated using the 11-box carbon cycle model (see 2.3), which suggests that the 1268–1269 CE event and the 1279–1280 CE event had occurred at the declining phase of the solar cycles, while the smallest event in 1261–1262 CE occurred at the maximum of the solar cycle. The solar cycle dependence of the events suggests that they were all caused by SPEs, rather than the galactic cosmic-ray enhancement mentioned above. The 1279–1280 CE event had occurred at the early stage of the declining phase, and the 1268–1269 CE event had occurred at the later stage of the declining phase. It is noteworthy that the timings of ground level enhancements (GLEs) captured by neutron monitors during the last 70 years have shown a similar tendency. GLEs are abrupt increases in cosmic-ray intensity associated with intense SPEs accompanying high-energy solar particles more than a few hundred MeV. The solar cycle dependence of the timings of GLE occurrence indicates that they increase as the number of sunspots increases, but they are also frequent during the declining phase of solar cycles (see Supplementary Figure S3). Note that GLE may also occur at the very end of the solar cycle, associated with sunspot activities at low-latitude regions, as was the case for the event of April 30, 1976 (Gopalswamy, 2012). A recent paper suggested that active regions with a multipolar configuration—having a high potential of triggering extreme solar flares—tended to occur at the solar activity maximum and the declining phase of the solar cycle during the recent two cycles (Solar Cycles 23 and 24) (Abramenko, 2021).

Interestingly, there has been a report of possible auroral activity on Feb 15th of 1269 CE in Korea (Abbott and Juhl, 2016). The record says that there was a white cloud with a width of 3 degrees spread across the sky at night. Due to the gradual change in the inclination angle of the geomagnetic field, it has been suggested that the auroral zone had been closer to the East Asia around the 13th century (Kataoka et al., 2021), and several aurorae were observed and recorded in Korea, China, and Japan. Photosynthesis of the asunaro tree is active from April to November and is most active around July to September (Hitsuma et al., 2012). Given that the asunaro tree mainly uses the photosynthate from around April to August for the growth of the correspondent year, a rapid jump from 1268 to 1269

CE does not contradict the time profile injection of protons in February of 1269 is assumed. No auroral activity has been found around 1279–1280 CE and 1261–1262 so far, except one suggested for Feb 9th of 1261 CE (Abbott and Juhl, 2016), which is too early for the carbon-14 peak in 1262 CE; but the solar cycle dependence of the events suggests that they were also caused by SPEs as mentioned above.

The evolution of solar cycles deduced from the high-precision carbon-14 suggests that the peak around 1275 CE had been significantly suppressed compared to the peak of the previous cycle. The end of the cycle then became extremely weakened, beyond the sunspot minimum of the modern period. As noted above, a sunspot level below zero implies a reduced solar activity more than can be probed by the number of sunspots. A previous study suggested that the Sun entered into the grand minimum state at around 1279 CE (Brehm et al., 2021): detailed analyses of carbon-14 improve the estimation, suggesting that the Wolf grand minimum had started around 1286 CE. It is noteworthy that the total length of the two solar cycles was approximately 27 years, suggesting a possibility that the length of the solar cycle had been longer than 11 years, as has been suggested as the common characteristics before the onset of the grand minimum (Miyahara et al., 2021), which is possibly associated with the reduction in the speed of meridional circulation in the solar convection layer, although further improvements to measurement precision are needed to precisely determine the duration of each solar cycle.

The reconstructed solar cycles with a drastically decreasing activity trend suggest that the SPEs found in this study had occurred during the transition time of solar activity into the grand minimum state. From the viewpoint of solar dynamo research, the Wolf minimum may provide a unique opportunity to discuss possible interactions between the solar dynamo and extreme solar flares. Large flares tend to occur at sunspots with complex topologies due to large available free energy (e.g., Sammis et al., 2000). The fact that there were large flares during the drastic transition phase of solar activity toward the Wolf minimum indirectly indicates that the toroidal magnetic field in the solar interior had been passive to the turbulent convection and was distorted significantly, leading to the generation of complex sunspots and large SPEs (see also Abramenko, 2021). In this regard, our results might constrain the status of the large-scale magnetic field and the convection in the solar interior. Our results may also provide an implication of the evolution of the Wolf minimum. Abramenko (2021) has shown that a large fraction of flaring active regions in the late phase of the cycle violates the dynamo rules (e.g., Hale's law). Nagy et al. (2017) argue that a single "rogue" active region, i.e., an anti-Hale large sunspot pair, can significantly affect the construction of the polar magnetic field in the following minimum and the amplitude of the subsequent solar cycle. The sunspot pairs that caused the SPEs discussed in this study, especially those associated with the 1268–1269 CE and the 1279–1280 CE events, might therefore have contributed to the generation of the Wolf minimum. The excavation of sunspot descriptions in historical documents may give further insight in this regard.

4. Conclusions

We found three recurrent carbon-14 increases in the tree rings of 1262 CE, 1269 CE, and 1280 CE just before the onset of the Wolf grand solar minimum. Analyses of the production rate suggest that the intensities of these events were ~14%, ~27 %, and ~19% of that of the 774–775 CE event. The solar cycles reconstructed around the events suggest that they had occurred at the solar cycle maximum or at the declining phase of solar cycles, consistent with the characteristics of large-sized solar flares observed during the modern period. It was suggested that they had occurred during a drastic transition time of solar activity. Further exploration of large-scale SPEs and a detailed reconstruction of solar cycles based on high-precision carbon-14 analyses may deepen our understanding of the nature of large-scale solar flares and their possible relation to the long-term variation of solar activity.

References

Shea, M. S., Smart, D. F., Allen, J. H., Wilkinson, D. C. (1992). Spacecraft problems in association with episodes of intense solar activity and related terrestrial phenomena during March 1991. IEEE Transactions on Nuclear Science, 39(6), 1754–1760. https://doi.org/10.1109/23.211363

Fujita, M., Sato, T., Saito, S., Yamashiki, Y. (2021). Probabilistic risk assessment of solar particle events considering the cost of countermeasures to reduce the aviation radiation dose. Scientific Reports, 11, 17091. https://doi.org/10.1038/s41598-021-95235-9

Lal, D., Peters, B. (1967). Cosmic ray produced activity on the earth. In: Sitte K. (ed.) Kosmische Strahlung II/cosmic rays II. Handbuch der Physik/Encyclopedia of Physics, vol 9/46/2. Springer, Berlin, Heidelberg. https://doi.org/10.1007/978-3-642-46079-17

Miyake, F., Nagaya, K., Masuda, K., Nakamura, T. (2012). A signature of cosmic-ray increase in AD 774-775 from tree rings in Japan. Nature, 486(7402), 240–242. https://doi.org/10.1038/nature11123

Miyake, F., Masuda, K., Nakamura, T. (2013). Another rapid event in the carbon-14 record of tree rings. Nature Communications, 4(1), 1748. https://doi.org/10.1038/ncomms287310.1038/ncomms2783

O'Hare, P., Mekhaldi, F., Adolphi, F., Raisbeck, G., Aldahan, A., Anderberg, E., et al. (2019). Multiradionuclide evidence for an extreme solar proton event around 2,610 BP (~660 BC). Proceedings of the National Academy of Sciences of the United States of America, 116(13), 5961–5966.

https://doi.org/10.1073/pnas.1815725116

Sakurai, H., Tokanai, F., Miyake, F., et al. (2020). Prolonged production of 14C during the ~660 BCE solar proton event from Japanese tree rings. Scientific Reports, 10, 660. https://doi.org/10.1038/s41598-019-57273-2

Maehara, H., Shibayama, T., Notsu, Y., Notsu, S., Honda, S., Nogami, D., et al. (2015). Statistical properties of superflares on solar-type stars based on 1-min cadence data. Earth, Planets and Space, 67, 59. https://doi.org/10.1186/s40623-015-0217-z

Brehm, N., Bayliss, A., Christl, M., Synal, H. A., Adolphi, F., Beer, J., et al. (2021). 11-year solar cycles over the last millennium revealed by radiocarbon in tree rings. Nature Geoscience, 14, 10–15. https://doi.org/10.1038/s41561-020-00674-0

Miyake, F., Panyushkina, I. P., Jull, A. J. T., Adolphi, F., Brehm, N., Helama, S., et al. (2021). A single-year cosmic ray event at 5410 BCE registered in 14C of tree rings. Geophysical Research Letters, 48, e2021GL093419.

https://doi.org/10.1029/2021GL093419

Schlamminger, L. (1990). Aurora borealis during the Maunder minimum. Monthly Notices of the Royal Astronomical Society, 247, 67–69.

Yamaguchi, Y. T., Yokoyama, Y., Miyahara, H., Sho, K., Nakatsuka, T. (2010). Synchronized northern hemisphere climate change and solar magnetic cycles during the Maunder minimum. Proceedings of the National Academy of Sciences of the United States of America, 107(48), 20697-20702. https://doi.org/10.1073/pnas.1000113107

Kataoka, R., Miyahara, H., Steinhilber, F. (2012). Anomalous 10Be spikes during the Maunder minimum: Possible evidence for extreme space weather in the heliosphere. Space Weather, 10, S11001, https://doi.org/10.1029/2012SW000835.

Miyahara, H., et al. (2004). Cyclicity of solar activity during the Maunder minimum deduced from radiocarbon content. Solar Physics, 224, 317–322

Kota, J., Jokipii, J. R., (1983). Effects of drift on the transport of cosmic rays. VI - A three-dimensional model including diffusion. Astrophysical Journal, 265, 573–581.

Miyahara, H., Tokanai, F., Moriya, T., Takeyama, M., Sakurai, H., Horiuchi, K., Hotta, H. (2021). Gradual onset of the Maunder Minimum revealed by high-precision carbon-14 analyses. Scientific Reports, 11, 5482. https://doi.org/10.1038/s41598-021-84830-5

Hakozaki, M. (2012). Dendrochronological study of coniferous buried forests in the late Holocene. Ph.D. Dissertation. Tohoku University, Sendai, Miyagi, Japan.(in Japanese)

Hakozaki, M., Nakamura, T., Ohyama, M., Kimura, J., Sano, M., Nakatsuka, T. (2016). Verification for the chronological age of woody remains from the Nitta (1) archaeological site in the Aomori city based on the AD774-775 14C-spike and δ18O dendrochronology. Nagoya paper XXVII, 34–39.

Tokanai, F., Kato, K., Anshita, M., Sakurai, H., Izumi, A., Toyoguchi, T., et al. (2013). Present status of YU-AMS system. Radiocarbon 55, 251–259.

Moriya, T., Takeyama, M., Sakurai, H., Umebayashi, T., Toyoguchi, T., Shiraishi, T., et al. (2019). Status of the AMS system at Yamagata University. Nuclear Instruments and Methods in Physics Research, B 439, 44–49.

Güttler, D., Adolphi, F., Beer, J., Bleicher, N., Boswijk, G., Christl, M., et al. (2015). Rapid increase in cosmogenic 14C in AD 775 measured in New Zealand kauri trees indicates short-lived increase in 14C production spanning both hemispheres. Earth and Planetary Science Letters, 411, 290–297.

Reimer, P., Austin, W., Bard, E., Bayliss, A., Blackwell, P., Bronk Ramsey, C., et al. (2020). The IntCal20 Northern Hemisphere Radiocarbon Age Calibration Curve (0–55 cal kBP). Radiocarbon, 62(4), 725–757. https://doi.org/10.1017/RDC.2020.41

Brehm, N., Christl, M., Adolphi, F., Muscheler, R., Synal, H. A., Mekhaldi, F., et al. Tree rings reveal two strong solar proton events in 7176 and 5259 BCE. Nature Communications, under review.

Gopalswamy, N. (2012). Energetic particle and other space weather events of solar cycle 24. In: Space weather: The space radiation environment: 11th Annual International Astrophysics Conference, AIP Conference Proceedings 1500, 14–19.

Abramenko, V. I. (2021). Signature of the turbulent component of the solar dynamo on active region scales and its association with flaring activity. Monthly Notices of the Royal Astronomical Society, 507, 3698–3706.

Abbott, D. H., Juhl, R. (2016). New historical records and relationships among 14C production rates, abundance and color of low latitude auroras and sunspot abundance. Advances in Space Research, 58, 2181–2246.

Kataoka, R., Nakano, S. (2021). Auroral zone over the last 3000 years. Journal of Space Weather and Space Climate, 11, 46. https://doi.org/10.1051/swsc/2021030

Hitsuma, G., Han, Q., Chiba, Y. (2021). Photosynthesis and growth of Thujopsis dolabrata var. hondai seedlings in the understory of trees with various phenologies. Journal of Service Research, 17, 156–163. http://doi.org/10.1007/s10310-011-0281-6

Sammis, I., Tang, F., Zirin, H. (2000). The dependence of large flare occurrence on the magnetic structure of sunspots. The Astrophysical Journal, 540, 583–587. https://doi.org/10.1086/309303

Nagy, M., Lemerle, A., Labonville, F., Petrovay, K., Charbonneau, P. (2017). The effect of “rogue” active regions on the solar cycle. Solar Physics, 292, 167. https://doi.org/10.1007/s11207-017-1194-0

Acknowledgments

We thank Ms. Yuka Yoshida for her assistance in the preparation of the cellulose samples. This work was supported by JSPS KAKENHI grand numbers 21H04497, 20H05643, 20H01369, and 19H00706.

Data Availability Statement

Datasets for this research are available at https://doi.org/10.6084/m9.figshare.17096975.v1.

Author Contributions

H.M. designed the study. H.M., F.T., T.M., M.T., and K.H. conducted the 14C measurements. M.O. performed the dating of tree-ring samples. H.M. and H.S. performed data analyses and modeling. H.M., H.H., and H.S. wrote the manuscript.

Competing Interest

The authors declare no competing interests.

Supplementary Information

Supplementary Information is available for this paper.

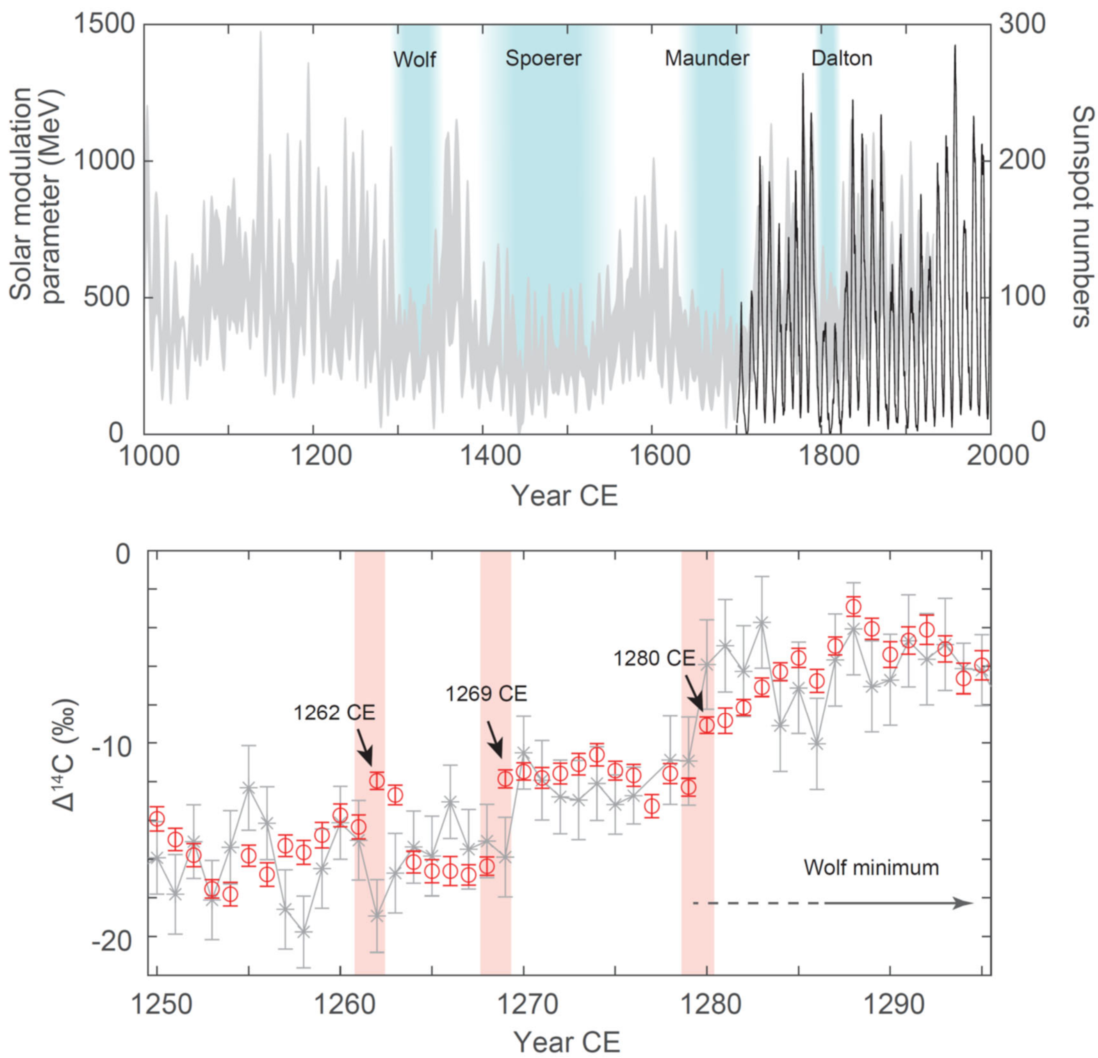

Figure 1. (a) Variation of solar modulation parameter for the past 1000 years reconstructed by Brehm et al. (2021). Blue shaded areas indicate periods of grand solar minima. (b) High-precision carbon-14 data for around the onset of the Wolf Minimum. Red circles are the carbon-14 data obtained in this study. Gray asterisks are the data by Brehm et al. (2021). Red shaded areas indicate the periods when statistically significant jumps in carbon-14 content were recognized.

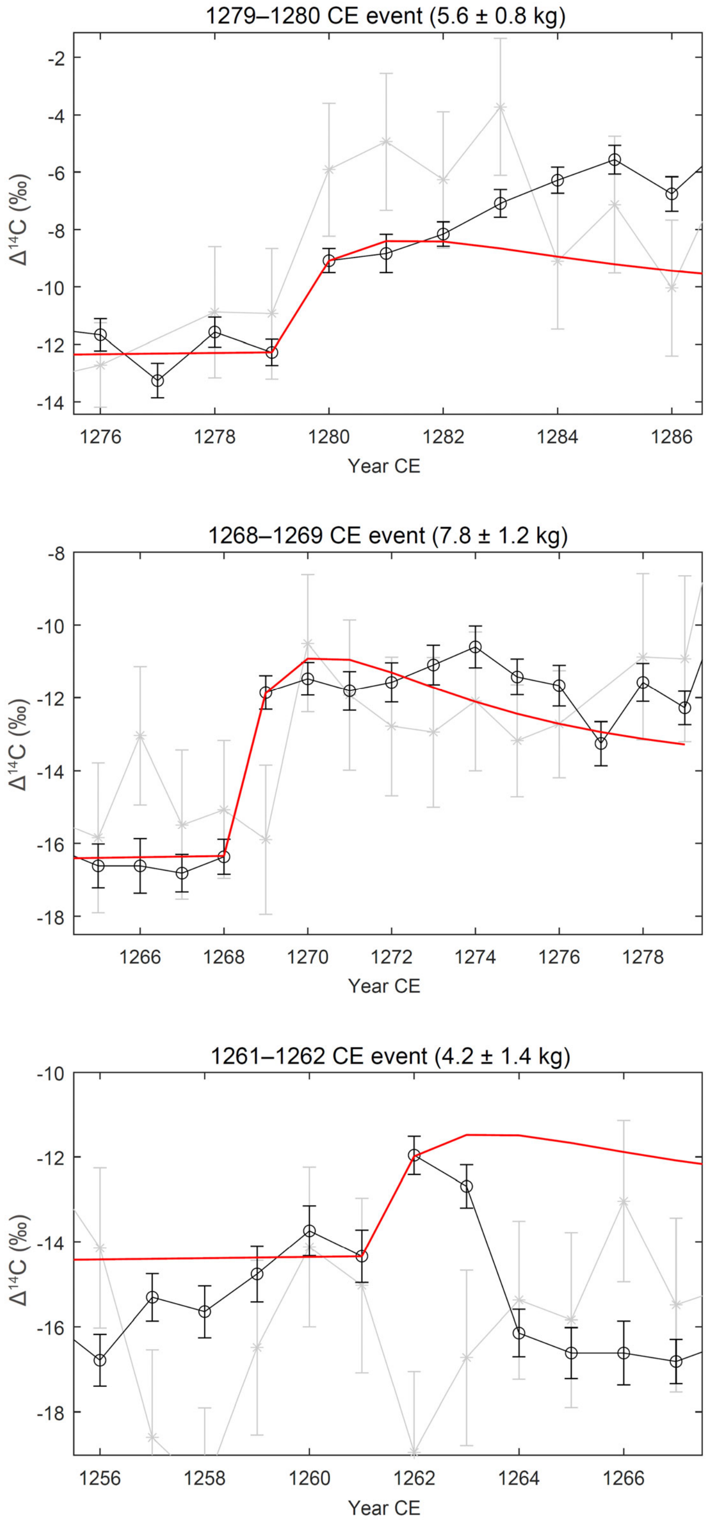

Figure 2. Time profile of carbon-14 content in tree rings around the SPE candidates: (a) 1279–1280 CE event, (b) 1268–1269 CE event, and (c) 1261–

1262 CE event. Black circles and gray asterisks are the carbon-14 data (same as in Figure 1b). Red lines show the response of carbon-14 content to the carbon-14 injections to the 11-box carbon cycle model. Note that solar cycle is not considered in this calculation.

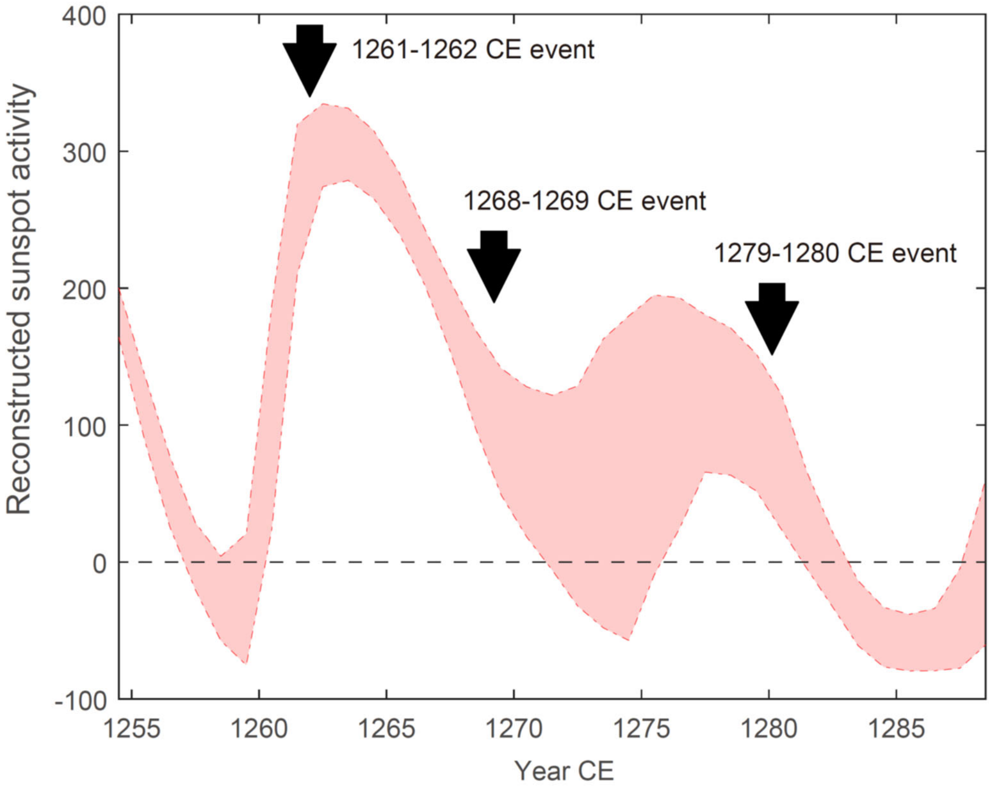

Figure 3. Reconstructed solar cycles around the carbon-14 enhancement events with an uncertainty range of 1.3 σ. Arrows indicate the approximate timing of the events found in this study.

[Geophysical Research Letters]

Supporting Information for

[Recurrent large-scale solar proton events before the onset of the Wolf grand solar minimum]

[Hiroko Miyahara[1,2], Fuyuki Tokanai[3,4], Toru Moriya[4], Mirei Takeyama[4], Hirohisa Sakurai[3], Motonari Ohyama[5], Kazuho Horiuchi[6], and Hideyuki Hotta[7]]

[[1]Humanities and Sciences/Museum Careers, Musashino Art University, Tokyo 187-8505, Japan, [2]Okinawa Institute of Science and Technology Graduate University, Okinawa 904-0495, Japan, [3]Faculty of Science, Yamagata University, Yamagata 990-8560, Japan., [4]Center for Accelerator Mass Spectrometry, Yamagata University, Yamagata 999-3101, Japan., [5]Botanical Gardens, Tohoku University, Miyagi 980-0862, Japan, [6]Graduate School of Science and Technology, Hirosaki University, Hirosaki, Aomori 036-8561, Japan., [7]Department of Physics, Graduate School of Science, Chiba University, 1-33 Yayoi-cho, Inage-ku, Chiba 263-8522, Japan]

Contents of this file

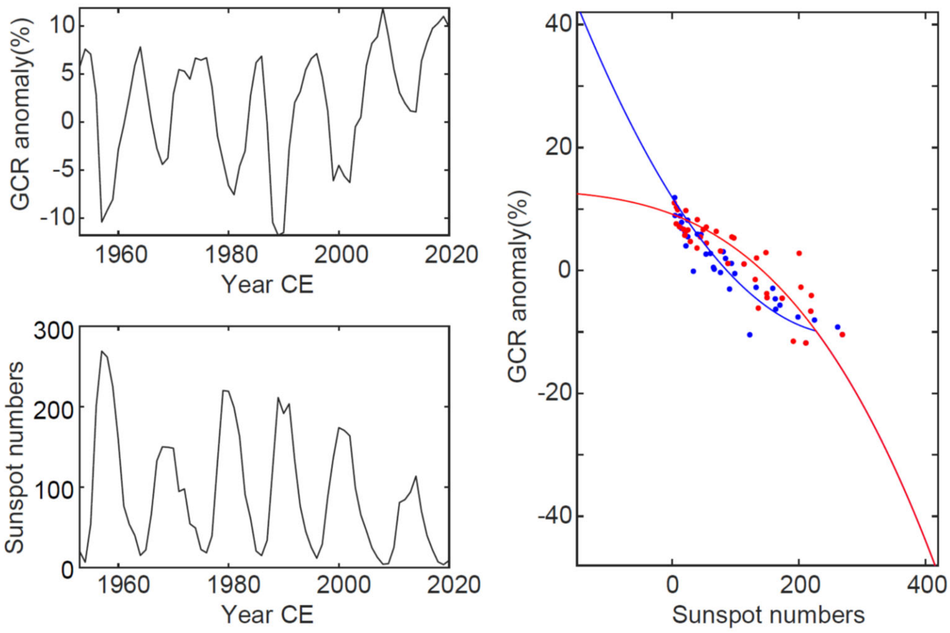

Figure S1. (a) Variation of galactic cosmic rays as monitored by the neutron monitors in Climax and Oulu stations. (b) Sunspot data from the World Data Center SILSO, Royal Observatory of Belgium, Brussels. (c) Comparison between the cosmic-ray flux and the sunspot numbers for the phases polarity of solar dipole magnetic field is positive (red dots) and negative (blue dots). The red and blue curves are the simple approximation and their extrapolation for sunspot numbers above 270 and below 0.

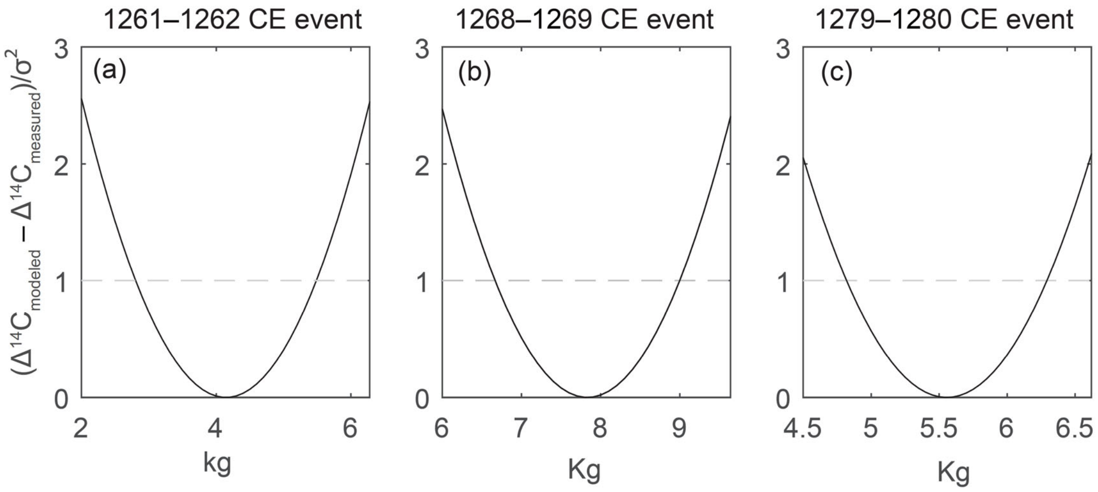

Figure S2. Comparison between the modeled and measured carbon-14 content for (a) 1261−1262 CE event, (b) 1268–1269 CE event, and (c) 1279–1280 CE event, for the cases carbon-14 was injected into the carbon cycle model within the ranges shown on the horizontal axes.

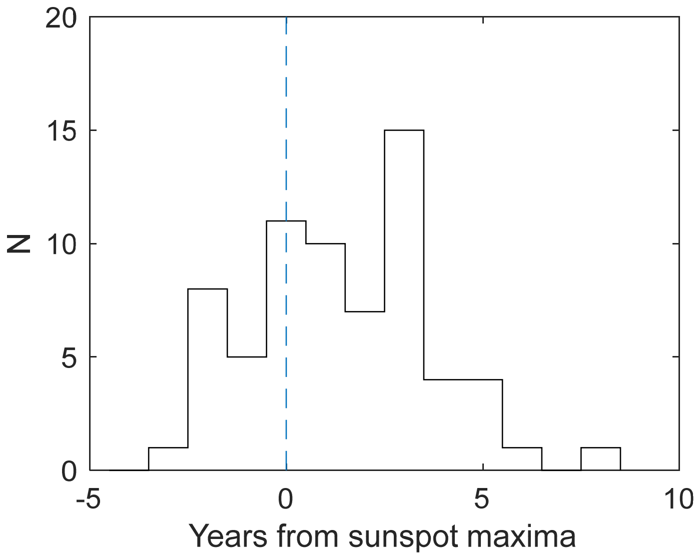

Figure S3. Solar cycle dependence of the number of ground level enhancements since 1956 CE.